

Article

Synthesis, Diagnosis and Study of Molecular Docking for 4-(4-amino-5-mercapto-4H-1,2,4-triazol-3-yl) Phenol and Its Coordination with Some Metals

Afraa Sabir Shihab

Department of Chemistry/ College of Education for Pure Sciences/ Tikrit University, Iraq

* Correspondence: afraasabir65@tu.edu.iq

Abstract: Triazol is an important nitrogen heterocyclic compound, containing three nitrogen atoms and two carbon atoms. Where triazole and its complexes were prepared by Acid Hydrazide (A1) was synthesis from the condensation of ester with hydrazine hydrate using ethanol absolute as a solvent. The next step involved the reaction of hydrazide acid, carbon sulfide (CS₂), and ethanol to produce oxadiazole (A2). Then, haydrazine hydrate was mixed with the triazole (A3) oxadiazole derivative. The complexes A4–A7 were produced by the reaction of the ligand (A3) with binary metal salts of the transition elements Co (II), Ni (II), Cu (II), and Mn (II). The reaction ratio of every complex that was produced was 1:1. The Ligand is Metal. The ligand was described using FT-IR, ¹H, ¹³C-NMR, and elemental analysis (C.H.N.S.M.). The generated compounds were diagnosed using infrared spectroscopy (FT-IR) techniques, magnetic sensitivity at ambient temperature, and other approaches. The results showed that the atoms of sulfur and nitrogen coordinate ligand bidentate. The form of the octahedral complex is as follows.

Keywords: Acid Hydrazide ,Oxadiazole, Triazol, , metal complex, Molecular Docking

Citation: Afraa Sabir Shihab. Synthesis, Diagnosis and Study of Molecular Docking for 4-(4-amino-5-mercapto-4H-1,2,4-triazol-3-yl) Phenol and Its Coordination with Some Metals Central Asian Journal of Theoretical and Applied Science 2024, 5(6), 543-554

Received: 10th Jul 2024
Revised: 11th Agt 2024
Accepted: 24th Sep 2024
Published: 17th Okt 2024



Copyright: © 2024 by the authors. Submitted for open access publication under the terms and conditions of the Creative Commons Attribution (CC BY) license (<https://creativecommons.org/licenses/by/4.0/>)

1. Introduction

Triazole is a heterocyclic organic nitrogen compound that is divided into isomers 1, 2, 3 – triazole and 1, 2, 4 – triazole. Triazole is prepared in many ways and as mentioned in the following sources [1-6]. Triazole has important applications due to its formation of bonds with enzymes and receptors that stimulate important biological activities such as antibacteria [7-10] and has uses anti-cancer [11], anti-tuberculosis [12, 13] and also Antidiabetic [14] and has study in agricultural chemistry and material chemistry [15-19]. Triazole was prepared in this study from interaction of oxadiazole with hydrazine aqueous and then attended complexes through the interaction of triazole with metal salts (Mn, Ni, Co, Cu) and formed complexes of octahedral shape and study of the Molecular Docking of some prepared compounds.

2. Materials and Methods

The study involved the synthesis of 4-(4-amino-5-mercapto-4H-1,2,4-triazol-3-yl) phenol and its coordination with metal salts of transition elements (Co(II), Ni(II), Cu(II), and Mn(II)). The synthesis process started with the preparation of the ligand through the reaction of oxadiazole with hydrazine hydrate. The synthesized ligand was then mixed

with metal salts to form complexes. The molar ratio of ligand to metal salt was maintained at 1:1 in all cases.

Characterization of the synthesized compounds was conducted using several techniques. Infrared spectroscopy (FT-IR) was employed to identify functional groups, and the presence of specific bands was indicative of successful complexation. Proton and Carbon-13 Nuclear Magnetic Resonance (^1H NMR and ^{13}C NMR) spectroscopy were used to confirm the molecular structure of the compounds. Magnetic susceptibility measurements were conducted at ambient temperature to investigate the coordination environment around the metal centers and determine the geometry of the complexes.

Additionally, molecular docking studies were performed using the MOE program. The protein target for docking was *Pseudomonas aeruginosa* (6R3X), and the docking scores and interactions between the synthesized compounds and the receptor were analyzed. The interactions included hydrogen bonds and π -type bonds with key amino acid residues. These experimental methods enabled the confirmation of the synthesis, characterization, and molecular interactions of the newly synthesized compounds with biological targets.

Experimental

Ester, hydrazine hydrate absolute ethanol (CHEM-LAB Company), Diethyl ether (Laboratory Rasayan Company). The salts of the transition metal elements, supplied from (MERCK Company), and were used without further purification. The melting points of compounds were determined in capillary tube using SMP30 melting point apparatus. Elemental analysis were carried out with a (Perkin Elmer-2400) The IR spectra were recorded on Shimadzu FT-IR (400-4000) cm^{-1} instrument using KBr. ^1H -NMR and ^{13}C -NMR spectra were recorded using DMSO as a solvent and TMS as internal standard, (Bruker 500) MHz instrument.

2.1 Synthesis of 4-hydroxybenzohydrazide (A_1) [20, 21]

One mole of ester and one mole of hydrazine hydrate were placed in a round-bottom flask, and twenty milliliters of 100% ethanol were added. After letting the mixture reflux for seven hours, it was cooled, the precipitate was filtered, washed with cold methanol, dried, and then ethanol was used to re-crystallize it. A white solid with a yield of 87% and a melting point of (256–258) $^\circ\text{C}$ was the end product. The ^1H -NMR spectra of the acid hydrazides are shown in Figure (4).

2.2 Synthesis of 4-(5-mercapto-1,3,4-oxadiazol-2-yl)phenol (A_2)

Added to the reaction vessel with the least quantity of water possible, (0.01) mole of A_1 and (0.01) mole of KOH dissolved in it contain (10) ml of 100% ethanol. In a cold water bath, (0.01) mole (2 ml) of CS_2 was added dropwise while stirring, and the mixture was refluxed for six hours. After adding ten milliliters of crushed ice and acidifying it with strong hydrochloric acid, the excess ethanol was distilled. The precipitate from (ethanol-water) was filtered, dried, and then crystallized again. The confirmation of the reaction completion was achieved by means of Thin-Layer Chromatography (TLC). The resultant substance was a white solid with a yield of 78% and a melting point of 220–222 $^\circ\text{C}$.

2.3 Synthesis of 4-(4-amino-5-mercapto-4H-1,2,4-triazol-3-yl)phenol (A_3)

Two moles (3.9 ml) of hydrazine hydrate and 0.01 mole (1.9 g) of A_2 were mixed with twenty milliliters of 100% ethanol. Once the liquid had cooled, it was combined with 25 milliliters of shattered ice and mixed thoroughly. After six hours of acidification with strong hydrochloric acid, the fluid was distilled to remove any remaining ethanol. After filtering, drying, and re-crystallizing from the ethanol, the precipitate was obtained. Thin-Layer Chromatography (TLC) was utilized to confirm the completion of the reaction. The finished product was a white solid with a melting point of (243–245) $^\circ\text{C}$ and a yield of 83%.

2.4 Synthesis of complexes (A_4 – A_5)

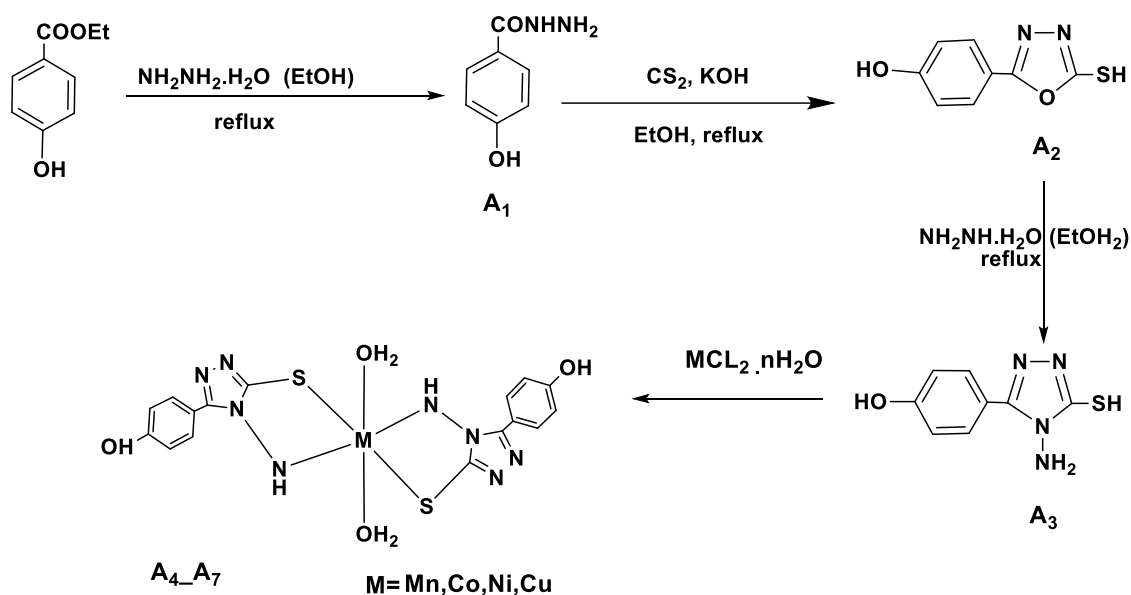
Ten milliliters of 100% ethanol, two moles of ligands, and one mole of each of the elemental salts (Ni+2, Cu+2, Co+2, and Mn+2) should be combined. Before recrystallizing with 100% ethanol, the mixture should be cooled, the precipitate filtered, and repeatedly rinsed with distilled water to get rid of any leftover salts. Five hours were spent stirring the mixture. To confirm that the reaction was proceeding as planned, physical attributes such as color and melting point were tracked (Table 1).

Table (1): Physical properties of the complexes A₄–A₇

Com. No.	Yield %	M.P.°C	Color	Cond. Ω ⁻¹ . M ²	Effective magnetic torque μ _{eff} (BM)
A4	78	263-265	pink	7.1	4.15
A5	84	276-278	Light violet	6.9	5.95
A6	88	275-277	Light green	8.1	3.31
A7	80	298-300	Light brown	7.5	2.12

3. Results and Discussion

The prepared organic compounds were characterized by melting point, Infrared spectroscopy (FTI-IR), elemental analysis (C.H.N, S), and nuclear magnetic resonance spectroscopy (H1, C13–NMR) . (C.H.N. S.M),



Scheme 1: The prepared compounds (A₁–A₇)

3.1 Infra - Red Spectra of the 4-hydroxybenzohydrazide (A₁)

The appearance of the stretching vibration of the carbonyl group (amide) at a lower frequency (1619) cm⁻¹ is the most well-characterized band in the infrared spectra of acid hydrazides. Another indication of the formation of acid hydrazides is the appearance of a strong peak at (3318) cm⁻¹ for the (–NH) group, which overlapped with the (–OH) phenolic.

3.2 Infra - Red Spectra of the 4-(5-mercapto-1,3,4-oxadiazol-2-yl)phenol (A₂)

A new peak for the (C=N) group appears at (1515) cm^{-1} , while the (C=S) group appears at (2590) cm^{-1} . The region (1268–1060) exhibits both symmetric and asymmetric (C–O–C) absorption bands.

3.4 Infra - Red Spectra of the 4-(4-amino-5-mercapto-4H-1,2,4-triazol-3-yl)phenol (A_3)

The appearance of symmetric and asymmetric (NH_2) absorption, as shown in Figure (1), and the elimination of symmetric and asymmetric (C–O–C) absorption in the range between (1066) cm^{-1} and (1268) cm^{-1} provide significant evidence for the formation of these compounds.

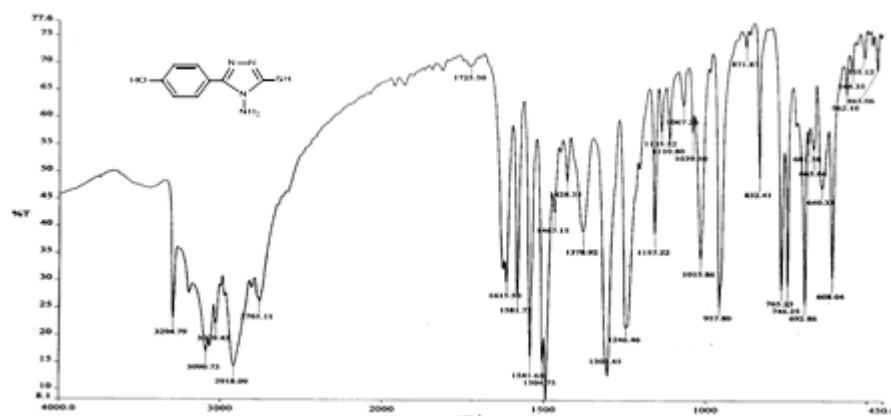


Fig. 1 Infrared Spectrum of the A_3 compound

3.5 Infra - Red Spectra of the 4-(4-amino-5-mercapto-4H-1,2,4-triazol-3-yl)phenol complexes (A_4 - A_7)

In addition to a bundle in the (450-414) cm^{-1} region representing the stretching of the metal bond with the sulfur atom in the pentagonal ring and another broad beam in the (3539-3326) cm^{-1} region corresponding to the stretching of the bond (O-H) in the water molecule involved in the complex structure, the complexes' spectra revealed new beams in the (973-946) cm^{-1} region that corresponded to the stretching of the metal bond with the nitrogen atom. The beam's width results from the creation of an interfacial hydrogen bond between water molecules. These new beams, as seen in Figures (2,3), represent the formation of complexes, metal bonds, sulfur atoms, and nitrogen. The infrared spectrum peaks (cm^{-1}) for the generated compounds (A_3 - A_7) are shown in Table (2).

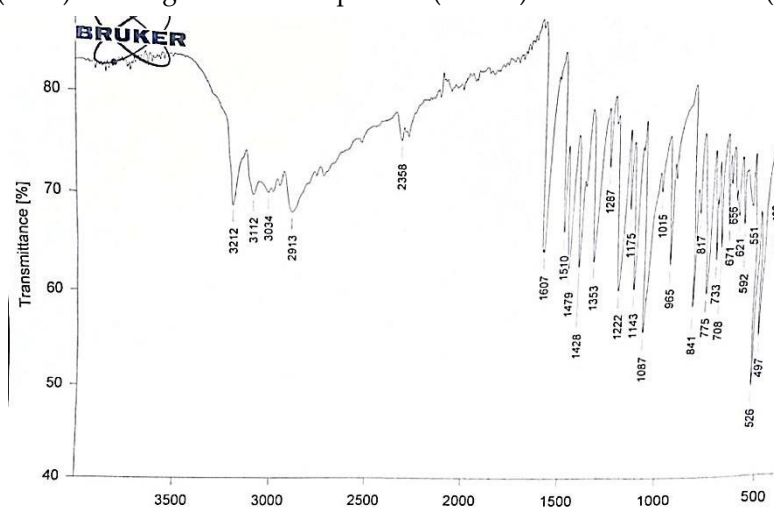


Fig. 2 Infrared Spectrum of the A_4 compound

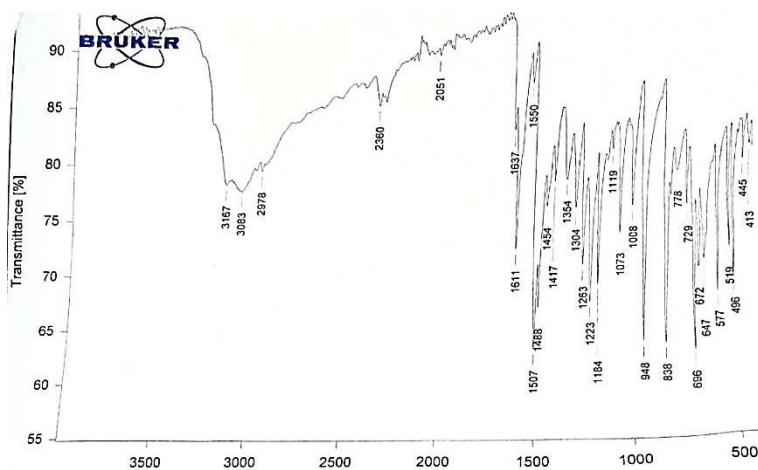


Fig.3 Infrared Spectrum of the A₇ compound

Table 2. IR Absorption Results (cm⁻¹) for compounds and complexes (A₁-A₆)

Comp. No.	O-H and / or N-H.	C=N	C-S	M-N	M-O	M-S	other
A ₁	3318	-	-				1619 C=O
A ₂	3300	1514	1170				1268, 1060 C-O-C Asy, Sym
A ₃	-	1612	1184	-			
A ₄	3439,3189	1600	1178	946	494	414	
A ₅	3212	1607	1175	966	497	418	
A ₆	3539,3115	1614	1170	965	490	415	
A ₇	3167	1611	1184	948	490	413	

3.6 (¹H, ¹³C -NMR) Spectroscopy of the 4-hydroxybenzohydrazide(A₁)

NMR spectra of this acid hydrazide show a broad weak singlet peak in (2.5) ppm integrating for two protons was assigned to (NH₂) protons. The group (-CO-NH-) proton exhibited singlet in (7.7) ppm, this chemical shift was due to the electron withdrawing field effect of neighboring (-CO-) group. The aromatic protons of the region (6.8-7.7) ppm, whereas the (O-H) protons of the phenolic group appeared as broad weak singlet at the (4.4) ppm as shown in Figure (4).

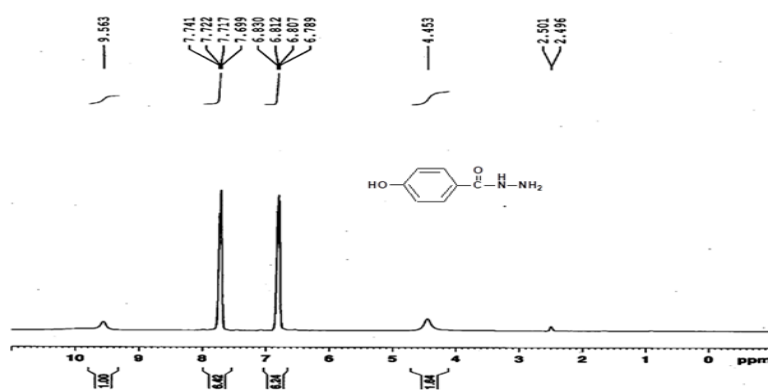


Fig. 4 of ^1H -NMR spectrum the compound A_1

3.7 (^1H , ^{13}C -NMR) Spectroscopy of the 4-(5-mercapto-1,3,4-oxadiazol-2-yl)phenol (A_2).

According to the ^1H NMR spectral data of oxadiazole, the dehydration cyclization reaction had taken place because the (O–H) protons of the phenolic group appeared as a broad weak singlet at the (4.4) ppm, while the (N–H) and (S–H) protons derived from tautomeric equilibrium resonated at the region (2.5–3.5) ppm as a broad singlet. The aromatic protons that appeared at 6.7–7.74 ppm are shown in Figure (5).

The carbon atom near SH is responsible for a signal that appeared at frequency ($\delta=177$ ppm), and the carbon atoms of the benzene ring are responsible for the signals at frequency ($\delta = 116\text{--}141$ ppm) that are displayed in Figure (6), according to an analysis of the ^{13}C -NMR spectrum of the prepared compound (A_2).

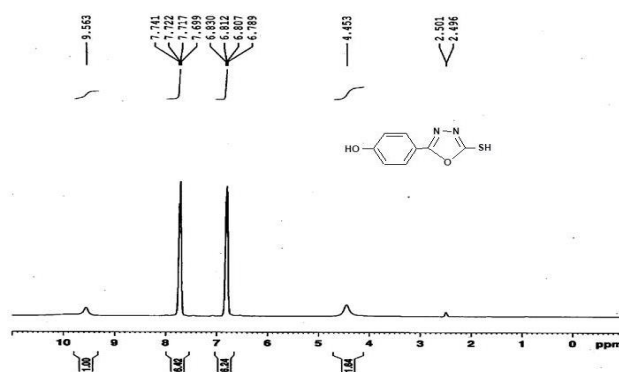


Fig. 5. ^1H -NMR spectrum of the compound A_2

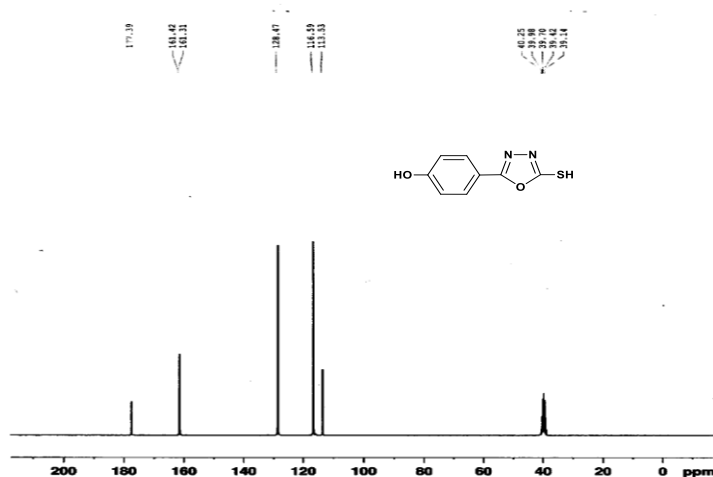


Fig. 6. ^{13}C -NMR spectrum of the compound A_2

3.8 (^1H , ^{13}C -NMR) Spectroscopy of the 4-(4-amino-5-mercapto-4H-1,2,4-triazol-3-yl)phenol (A_3).

The triazole ^1H -NMR spectra are summarized in table (3-8) where the (N–H) and (S–H) tautomeric protons are observed in the area (2.5–3.5) ppm, while the (O–H) protons of the phenolic group appeared as a broad weak singlet at (5.7) ppm. The aromatic protons in the 6.8–7.68 ppm range are depicted in Figures (7). Analyzing the (A_3) ^{13}C -NMR spectra of the generated compound, it was seen that, as shown in Figure (8), the carbon atoms in

the benzene ring are responsible for signals at ($\delta = 115-159$ ppm), whereas the carbon atom next to SH is responsible for a signal at frequency ($\delta=166$ ppm).

Fig. 7 ^1H -NMR spectrum of the compound A_3

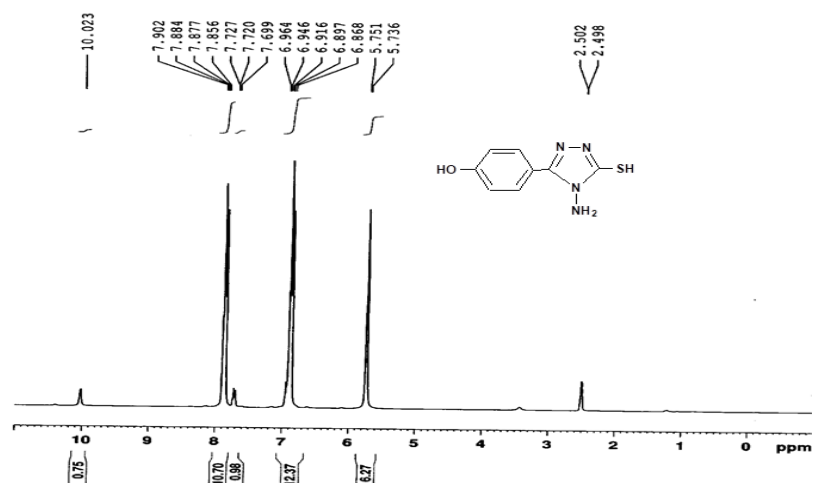
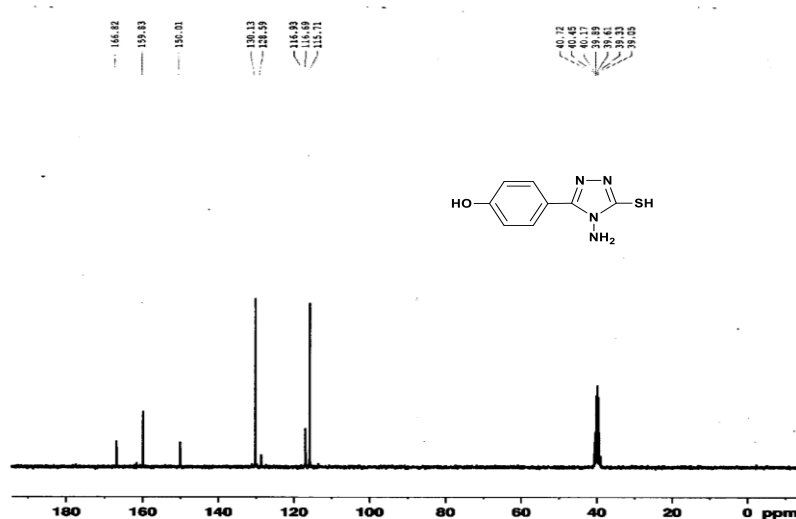


Fig.8 ^{13}C -NMR spectrum of the compound A_3



3.9 Molar electrical conductivity of Prepared Complexes (A_4 - A_7)

In this study, the molar electrical conductivity of the complexes was measured at a concentration of (10^{-3}) molar by using absolute ethanol as a solvent after allowing the solution to be in thermal equilibrium at room temperature, through molar electrical conductivity measurements, we find that it is consistent with the proposed formula for complexes, where we found that the conductivity is low, meaning that the solutions of non-electrolytic complexes so that we do not have molecules with high polarity such as water or ions, All the data were shown in Table (1).

3.10 Magnetic Measurements of Prepared Complexes (A_4 - A_7)

The magnetic susceptibility of the resulting complexes was measured at 25°C . The diamagnetic corrections (D) for the atoms in the organic molecules, metal ions, and non-organic radicals were applied using Pascal's constants for the component atoms of the generated complexes. The effective magnetic moment (μ_{eff}) of the complexes was

calculated using magnetic measurements of the generated Mn (II) and Co(II). Ni (II) and Cu (II) complexes (A3-A7) These results suggest that the metallic (II) ion possesses an octahedral high-spin shape with sixes coordination. All of the data were shown in Table 1 (1).

3.11 Elemental Analysis (C.H.N. S.M).

In order to ascertain the composition of the synthesized compounds (A3-A7), confirm their validity, and calculate the practical percentage with respect to the theoretical % for each compound, elemental analysis (C.H.N.S.M.) was utilized. All of the data were shown in Table 3.

Table 3. Elemental analysis of the compounds (A₃-A₇)

No	Formula	(Calculated) theoretical %				
		C	H	N	S	M
A ₃	C ₈ H ₈ N ₄ OS	(46.2) 46.14	(3.91) 3.87	(26.9) 26.91	(15.4) 15.40	-
A ₄	[Mn(A ₃) ₂ (H ₂ O) ₂]	(38.19) 38.17	(3.24) 3.20	(22.28) 22.26	(12.76) 12.74	(10.95) 10.91
A ₅	[Co(A ₃) ₂ (H ₂ O) ₂]	(37.89) 37.87	(3.19) 3.18	(22.11) 22.08	(12.67) 12.64	(11.63) 11.61
A ₆	[Ni(A ₃) ₂ (H ₂ O) ₂]	(37.91) 37.89	(3.21) 3.18	(22.12) 22.09	(12.56) 12.54	(11.58) 11.57
A ₇	[Cu(A ₃) ₂ (H ₂ O) ₂]	(37.55) 37.53	(3.17) 3.15	(21.91) 21.88	(12.54) 12.52	(12.45) 12.4

3.12 Molecular Docking [22, 24]

In order to obtain the most stable vacuum form (the least disabled energy), the molecular docking of some prepared compounds (A3, A5, A7) was studied on one line, which is the bacteria *Pseudomonas aeruginosa*, using the MOE program. After that, the protein composition of *Pseudomonas aeruginosa* bacteria was downloaded from the World Bank website for receptor 6R3X, and a personal calculator was used. whereby the binding energies of the compounds were calculated and displayed in Table (4). The number and kinds of bonds that these prepared derivatives establish with amino acid residues located in the active site by forming a number of bonds were determined by studying the molecular fusion of prepared organic derivatives [25].

Table (4) Binding energy values and RDMS values between prepared compounds and receptor (6R₃X) one line of *Pseudomonas aeruginosa*

NO.	Complex	Docking Score (kcal/mol)	RMSD (A°)
A ₃	C ₈ H ₈ N ₄ OS	-4.375	3.287
A ₅	[Co(A ₃) ₂ (H ₂ O) ₂]	-6.727	1.514
A ₇	[Mn(A ₃) ₂ (H ₂ O) ₂]	-6.287	1.142

The investigation revealed that the compound (A3) interacts with the amino acid residues that are present in the active site by creating two different kinds of bonds: a hydrogen bond that connects the amino acid residue Lys.348 in the active site with the nitrogen atom of the amine group's electron pair and a length of (2.16 Å); a π type bond that binds the amino acid Ser.485 to the benzene ring; and a π type bond that binds the amino acid Ser.349 to the triazole ring. Other amino acids that are impacted by the Vandervaalz forces are listed in Table (4) above.

Figure (9) displays the interaction between the synthesized chemical (A3) and the 6R3X receptor (*Pseudomonas aeruginosa*) as well as the two- and three-dimensional representation of the molecular anchoring results.

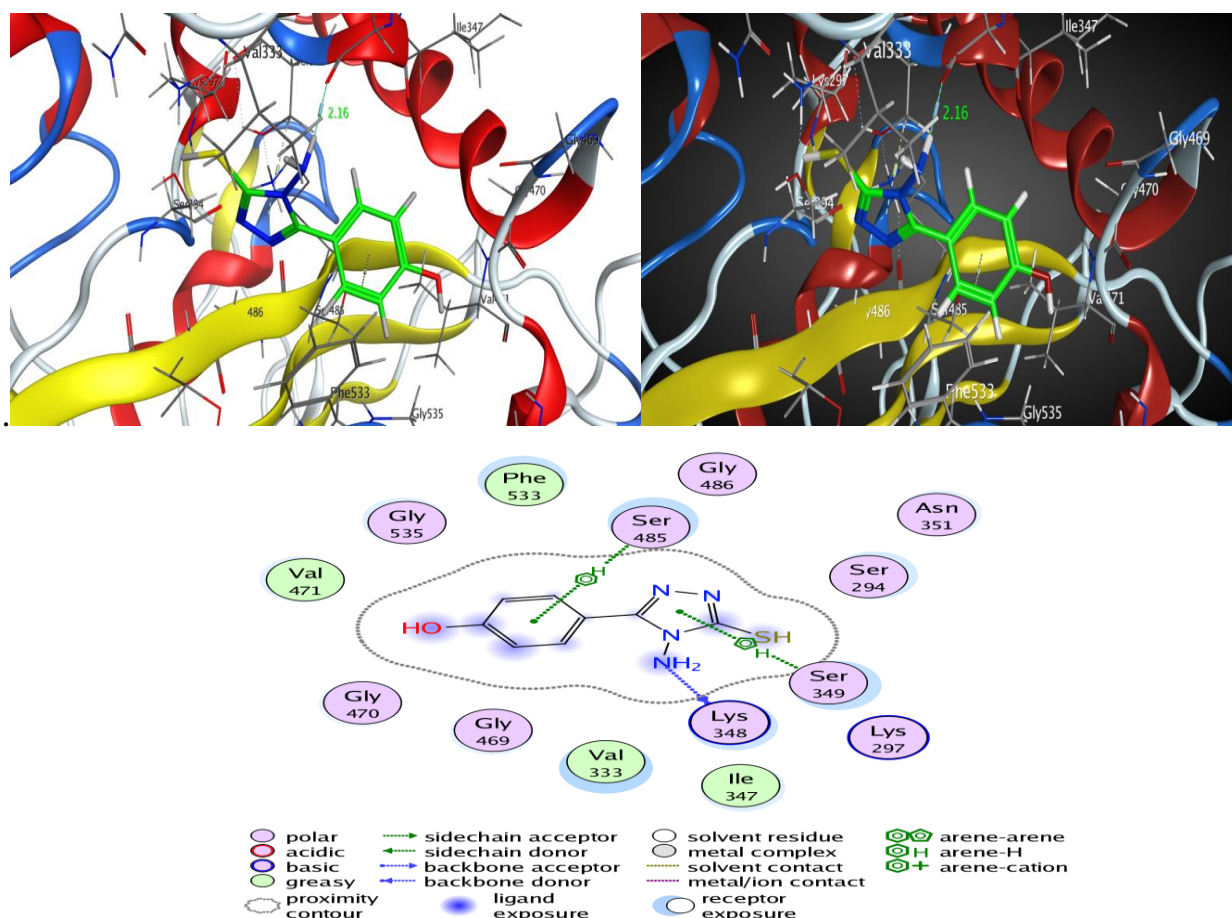


Fig. 9. Interactions of A₃ and receptor 6R₃X

The study reports that the molecule (A5) forms two distinct kinds of hydrogen bonds with amino acid residues found in the active region. First, amino acid Arg.489 is bound to the benzene ring via a π type bond. Several other amino acids were found to be impacted by Vanderphals forces, and binding energy values were determined; these are mentioned in Table (1) above. Secondly, the active site amino acid residue Tys.348 is connected to the oxygen atom hydroxyl group electron pair via a length of (2.39 Å). The relationship between the synthetic chemical (A5) and the *Pseudomonas aeruginosa* bacterium's receptor 6R3X one line is shown in Figure (2), along with a two- and three-dimensional depiction of the molecular anchoring outcomes.

Figure (10) depicts the interaction between the synthesized chemical (A5) and the 6R3X receptor (*Pseudomonas aeruginosa*) as well as the two- and three-dimensional representation of the molecular anchoring results.

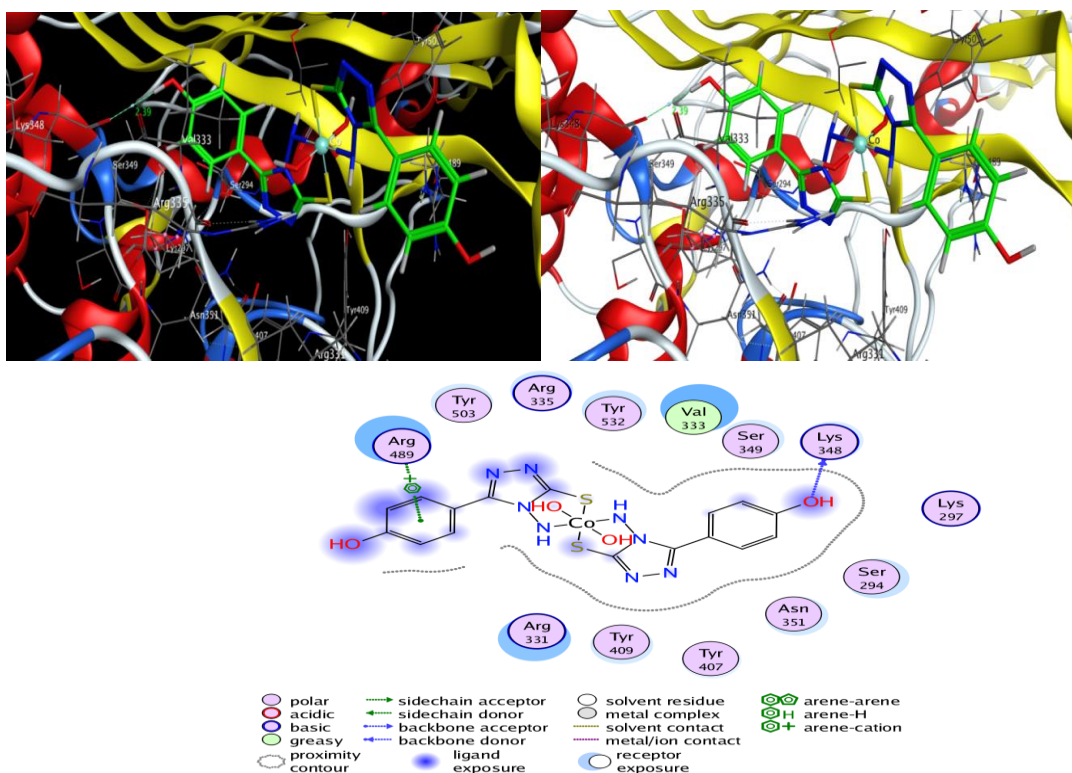
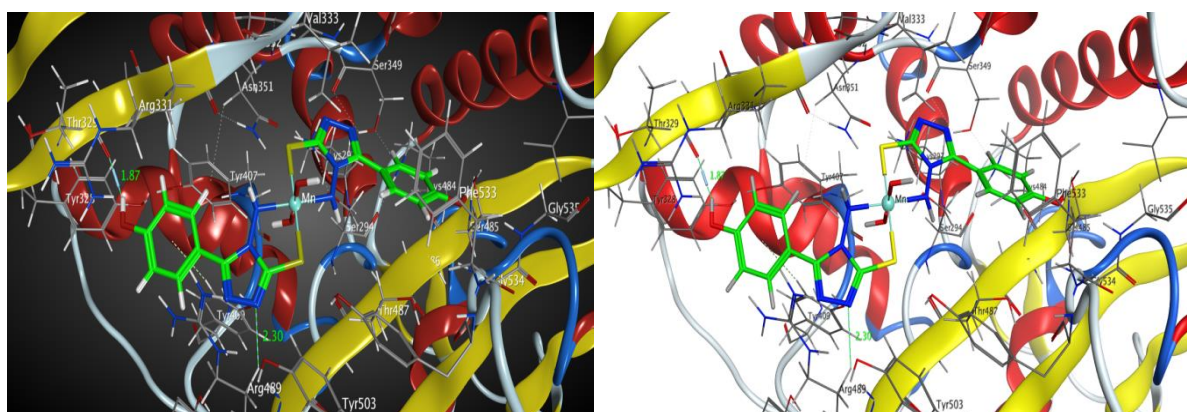


Fig. 10. Interactions of A₅ and receptor 6R₃X

The study found that when the compound (A7) interacts with amino acid residues found in the active site, it forms two distinct types of bonds: hydrogen bonds that link amino acid residue Thr.329 to the oxygen atom hydroxyl group electron pair with a length of (1.87 Å) and hydrogen bonds that link amino acid residue Arg.331 to the oxygen atom. A variety of amino acids were affected by the Vanderphals forces, and the binding energy values were determined as shown in Table (1) above. This molecule, which has an electron pair of sulfur atoms with a length of 2.30 Å and a type π bond, is connected to the benzene ring through Tyr.409.

Figure (11) depicts the association between the synthesized chemical (A7) and the *Pseudomonas aeruginosa* receptor 6R3X, one line, as well as the two- and three-dimensional representation of the molecular anchoring results.



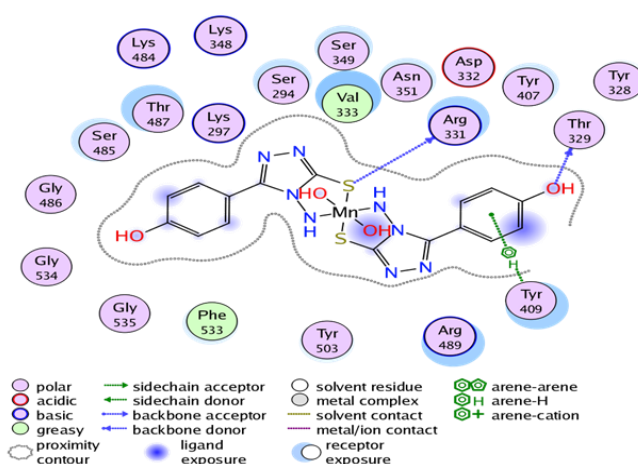


Fig. 11. Interactions of A₇ and receptor 6R₃X

4. Conclusion

Compound (A₃) easily forms complexes, especially with Mn (II), Co (II), Ni (II) and Cu (II) salts. The complexes exhibit an octahedral geometry in this study. The prepared compounds and their complexes exhibited high stability and strength, maintaining their structure, color, and melting point even under varying laboratory temperatures. This review outlined the triazoles complexes served as a resource for both basic and applied research on the subject, which is of significant importance since the parent compounds are used as pharmaceuticals in the medical field.

REFERENCES

- [1] Zhan-Jiang Zheng, Ding Wang, Zheng Xu and Li-Wen Xu..synthesis of bis-1,2,3-triazoles by copper-catalyzed Huisgen cycloaddition: A family of valuable products by click chemistry Beilstein J. Org. Chem. 11, 2557–2576(2015)
- [2] Nageswara Rao G. Synthesis of triazoles and their derivatives by treating with hydrazine hydrate, thiocarbohydrazide and thiosemicarbazide: A review. Journal of Research in Chemistry 5(1): 151-155, (2024).
- [3] Rodrigo Octavio M.M.A. Desouza and Leandros Demrizmeriranda. Strategies Towards the Synthesis of N2-Substituted 1,2,3-Triazoles. Anais da Academia Brasileira de Ciências 91 (Suppl. 1): e20180751, (2019).
- [4] Vala P., Ruturajsinh M. Vala, and Hitendra M. Patel, Versatile Synthetic Platform for 1,2,3-Triazole Chemistry Disha. ACS Omega, 7, 36945–36987 (2022).
- [5] Jinlian Dai, Sen Tian, Xueqing Yang and Zongliang Liu, Synthesis methods of 1,2,3-/ 1,2,4-triazoles: A review. Frontiers in Chemistry- ISHED 26 September (2022).
- [6] Strzelecka, M., and Swiatek, P. Triazoles as Important Antibacterial Agents. Pharmaceuticals (Basel) 114, 24. (2021).
- [7] (Review article) AJPS (2022) 65 Synthesis and Biological Activities of Some 1,2,4-Triazole Derivatives: A Review Dina Saleem M. Ameen, Mohammed Dheyaa Hamdi, Ayad Kareem Khan, Al Mustansiriyyah Journal of Pharmaceutical Sciences, Vol. 22, No.3, (2022).
- [8] Ana Luisa M. Morotti and Karen Luise Lang - Semi-Synthesis of new glycosidic triazole derivatives of dihydrocucurbitacin. Tetrahedron Letters 56 (2 January (2015).
- [9] Mohammed M. Matin, Priyanka Matin, Rezaur Rahman, Triazoles and Their Derivatives: Chemistry, Synthesis, and Therapeutic Applications. Frontiers in Molecular Biosciences, 25 April 2022 | www.frontiersin.org 2 Volume 9 April (2022).

- [10] Sujana Oggu, Parameswari Akshinthala, LaxmiKumari Nagarapu, Srimannarayana Malempati. Design, synthesis, anticancer evaluation and molecular docking studies of 1,2,3-triazole incorporated 1,3,4-oxadiazole-Triazine derivatives. *Heliyon*, Volume 9, Issue 5, May 2023, e15935.
- [11] Anindra Sharma, Anand K. Agrahari, Sanchayita Rajkhowa, Vinod K. Tiwari. Emerging impact of triazoles as anti-tubercular agent. *Eur. J Med Chem.* 2022 Aug 5;238:114454. - PubMed doi: 10.1016/j.ejmech.2022.114454.
- [12] Jayati Nandi and Sankar V. K., Synthesis and Docking of the Schiff base derived from 4-aminopyridine. *JPSI*: 1(5), 9-11, (2012).
- [13] Fallah, Z., Tajbakhsh, M., Alikhani, M., Larijani, B., FarAMARZI, M. A., Hamedifar, H., et al. A review on synthesis, mechanism of action, and structure-activity relationships of 1,2,3-triazole-based α -glucosidase inhibitors as promising anti-diabetic agents. *J. Mol. Struct.* 1255, 132469. (2022).
- [14] Bharghavi Chintaa and Ramakrishna Chintalapudi. Sulfated Tin Oxide (STO)-Catalyzed Efficient Synthesis of 4-Aryl-NH-1,2,3-triazoles. *Current Chemistry Letters* 13, 669–676, (2024).
- [15] Adnan Ibrahim Mohammed, Synthesis of Nonionic Surfactants. Sugar-Substituted Ether-Linked Bis-1,2,3-Triazoles, *Asian Journal of Chemistry*; Vol. 24, No. 12, 5585-5588 (2012).
- [16] Shahad Muhammad and Ahmed Ahmed. Synthesis, characterization and photostability study of triazole derivatives. *GSC Advanced Research and Reviews*, 09(02), 066–072 (2021).
- [17] Jyotirmoy Ghosh and R. Graham Cooks. Facile Synthesis of Triazoles using Electrospray-Deposited Copper Nanomaterials to Catalyze Azide-Alkyne Cycloaddition (AAC) Click Reactions. *ChemPlusChem*, 87, e202200252 (1 of 6) (2022).
- [18] Arianna Rossetti, Alessandro Sacchetti, Fiorella Meneghetti, Greta Colombo Dugoni, Matteo Mori and Carlo Castellano. Synthesis and Characterization of New Triazole-Bispidinone Scaffolds and Their Metal Complexes for Catalytic Applications. *Molecules*, 28, 6351, (2023).
- [19] Abdul Hameed A., Hassan F. Synthesis, Characterization and Antioxidant Activity of Some 4-Amino-5-phenyl-4H-1,2,4-triazole-3-thiol Derivatives. *Int. J. App. Sci. Tech*: 4 (2), 202-211, (2014).
- [20] Abdelhamid, A. A., Salah, H. A., & Marzouk, A. A. Synthesis of imidazole derivatives: Ester and hydrazide compounds with antioxidant activity using ionic liquid as an efficient catalyst. *Journal of Heterocyclic Chemistry*, 57(2), 676-685. (2020).
- [21] Hashem H.E., Nath A., Kumer A. Synthesis, molecular docking, molecular dynamic, quantum calculation, and antibacterial activity of new Schiff base-metal complexes. *Journal of Molecular Structure*, V. 1250, 131915 (2022).
- [22] Mashood Ahamed F.M., Shakya B., Shakya S. Synthesis and characterization of a novel Mannich base benzimidazole derivative to explore interaction with human serum albumin and antimicrobial property: experimental and theoretical approach. *Journal of Biomolecular Structure and Dynamics*, V. 41(18), p. 8701–8714 (2022).
- [23] Shihab A.S. Synthesis, Diagnosis, Evaluation of Biological Activity and Study of Molecular Docking for Furosemide Derivative and Its Coordination with Some Metals. *Chemical Problems*, V. 22 (3), p. 312-322. (2024).
- [24] Kogut M.M., Marcisz M., Samsonov S.A. Modeling glycosaminoglycan–protein complexes. *Current Opinion in Structural Biology*, V. 73, 102332, (2022).